Exogenous Fatty Acids Remodel *Staphylococcus aureus* Lipid Composition through Fatty Acid Kinase

Zachary R. DeMars[a], Vineet K. Singh[b] and Jeffrey L. Bose [a#]

[a]Department of Microbiology, Molecular Genetics and Immunology, University of Kansas Medical Center, Kansas City, Kansas, USA

[b]Department of Microbiology and Immunology, A.T. Still University of Health Sciences, Kirksville, Missouri, USA

Running Head: Utilization of exoFAs Influences *S. aureus* Membranes

[#]Address correspondence to Jeffrey L. Bose, jbose@kumc.edu

Key words: lipidomics, MRSA, phospholipid membranes

Abstract

Staphylococcus aureus can utilize exogenous fatty acids for phospholipid synthesis. The fatty acid kinase FakA is essential for this utilization by phosphorylating exogenous fatty acids for incorporation into lipids. How FakA impacts the lipid membrane composition is unknown. Here, we used mass spectrometry to determine the membrane lipid composition and properties of *S. aureus* in the absence of *fakA*. We found the *fakA* mutant to have increased abundance of lipids containing longer acyl-chains. Since *S. aureus* does not synthesize unsaturated fatty acids, we utilized oleic acid (18:1) to track exogenous fatty acid incorporation into lipids. We observed a concentration-dependent incorporation of exogenous fatty acids into the membrane that required FakA. We also tested how FakA and exogenous fatty acids impact membrane-related physiology and identified changes in membrane potential, cellular respiration, and membrane fluidity. To mimic the host environment, we characterized the lipid composition of wild-type and *fakA* mutant bacteria grown in mouse skin homogenate. We show that wild-type *S. aureus* can incorporate exogenous unsaturated fatty acids from host tissue highlighting the importance of FakA in the presence of host skin tissue. In conclusion, FakA is important for maintaining the composition and properties of the phospholipid membrane in the presence of exogenous fatty acids, impacting overall cell physiology.

Importance

Environmental fatty acids can be harvested to supplement endogenous fatty acid synthesis to produce membranes and circumvent fatty acid biosynthesis inhibitors. However, how the inability to use these fatty acids impacts lipids is unclear. Our results reveal lipid composition changes in response to fatty acid addition and when *S. aureus* is unable to activate fatty acids through FakA. We identify concentration-dependent utilization of oleic acid, that when combined with previous

work, provides evidence that fatty acids can serve as a signal to *S. aureus*. Furthermore, using mouse skin homogenates as a surrogate for *in vivo* conditions, we show that *S. aureus* can incorporate host fatty acids. This study highlights how exogenous fatty acids impact bacterial membrane composition and function.

Introduction

Despite decades of intense research, *Staphylococcus aureus* remains a tremendous cause of infection and morbidity in the human population (1). Approximately 30% of the population are asymptomatic carriers of *S. aureus* (2); however, this bacterium can cause infection in numerous anatomical sites, including skin and soft tissues, bones, lungs, hearts, as well as foreign implants such as catheters and prosthetic joints (3). Originally characterized as a typically hospital-acquired infection, the incidence of infections in the community has increased concern and awareness of this pathogen as community-associated strains have become dominant in the US (4, 5). Thus, a thorough understanding of how *S. aureus* can establish infection, fend off the immune system, and maintain infection is needed to combat this pathogen.

Phospholipids lie at the interface of the host-pathogen interaction. Membrane associated products, such as lipopolysaccharides, lipoteichoic acids, and lipoproteins are sensed by the germ-line encoded pattern-recognition receptors that induce the activity of numerous host immune cells (6, 7). In addition to these membrane products, phospholipids themselves can play a role in evading the immune system. For example, lysyl-phosphatidyl glycerol (LPG) has been shown to be important for evading neutrophils and antimicrobial peptides (8, 9). The composition of the phospholipid membranes of bacteria can also dictate if antimicrobial treatment during infection is successful. Resistance to daptomycin, a lipopeptide antimicrobial, can result from the mutation of cardiolipin synthase (*cls2*) and increased abundance of cardiolipin (10). Microbial lipids can also

serve as antigens for the immune system (11), further emphasizing the role that lipids play during the infection process. More recently, the identification of bacterial extracellular vesicles has also become a topic of interest and could contribute to host-pathogen interactions (12). These data clearly suggest that the composition of the phospholipid membrane is a vital component of the host-pathogen interface.

Synthesis of lipids is preceded by the production of fatty acids. *S. aureus* endogenously synthesizes fatty acids via the fatty acid synthesis type II system (FASII) (13). Due to the differences between fatty acid synthesis enzymes of bacteria from humans, FASII has been the subject for antimicrobial targets (14-17). Bacteria, including *S. aureus*, can supplement endogenous fatty acid synthesis by utilizing exogenous fatty acids (exoFAs) (18). These exoFAs are predicted to passively diffuse into the phospholipid membrane. In *S. aureus*, exoFAs are thought to be removed from the membrane by fatty acid-binding proteins FakB1 and FakB2 (18). Once removed from the membrane, fatty acid kinase, FakA, then phosphorylates the carboxyl head group of the fatty acid creating an acyl-phosphate (18) that can then be used for lipid synthesis. *S. aureus* predominantly synthesizes three classes of phospholipids: phosphatidylglycerol (PG), lysl-phosphatidylglycerol (LPG), and cardiolipin (CL) (8, 19). One interesting caveat to fatty acid and lipid synthesis in *S. aureus* is the inability of this bacterium to synthesize unsaturated fatty acids (20). Instead, *S. aureus* utilizes branched-chain fatty acids (BCFAs), derived from the branched-chain amino acids isoleucine, leucine, and valine, to help modulate the membrane in response to environmental stimuli (21, 22). A large portion of the BCFAs produced by *S. aureus* include odd-numbered iso and anteiso BCFAs, with acyl-chain length of 15 being the most abundant (22, 23).

FakA was first identified as a regulator of virulence due to the decrease in α-hemolysin activity, increased protease activity, and increased dermonecrosis in a murine model of infection (24).

Originally named virulence factor regulator B, VfrB, due to this altered virulence, FakA was eventually identified to be a fatty acid kinase important for phosphorylating exoFAs (18). Subsequently, the altered virulence factor profile of a *fakA* mutant was identified to be due, in part, to altered activity of the SaeRS two-component system (25, 26). The current model for the FakA-dependent alteration of SaeRS signaling is due to the accumulation of fatty acids within the cell (26). A mechanism for how these accumulated fatty acids within the cell decreases SaeRS signaling is still at large. The absence of FakA affects global metabolism (27) and increases the resistance of *S. aureus* to toxic fatty acids (28, 29).

How the inability to use exoFAs affects the overall membrane lipid composition has not been evaluated. In the current study, we aimed to determine the changes in membrane lipid composition in the absence of FakA. We tested how these overall membrane lipid changes affect the properties of the membrane itself. Lastly, we provide evidence that *S. aureus* grown in the presence of host tissue can use unsaturated fatty acids to supplement phospholipid synthesis, extending our observations from standard laboratory media to include fatty acids found in murine skin. These results increase the importance that the fatty acid utilization system has in the presence of host-derived tissues.

Results

Cellular and extracellular fatty acid profile of *fakA* mutant. FakA is necessary for *S. aureus* to incorporate exoFAs into acyl chains of membrane lipids. Thus, it would be expected that the absence of FakA would alter the abundance of FAs in the cell. Indeed, a previous study determined that a *fakA* mutant accumulates fatty acids (26). Our studies are typically performed in TSB and therefore we sought to recapitulate this accumulation of fatty acids at different phases of growth in the *fakA* mutant under our growth conditions and our *S. aureus* strain of choice, AH1263, a

derivative of the USA300 strain LAC. Using LC/MS/MS, we quantified the available free fatty acids in TSB and found that 16:0 and 18:0 constitute the most abundant fatty acids (Figure S1). Next, we determined how FakA affects fatty acid pools. To this end, the free fatty acid profiles of cellular and extracellular fatty acids for wild type and *fakA* mutant was determined. This was tested at two-time points representing early (3 hours) and late (6 hours) exponential phase of growth, times that we have previously characterized the metabolic changes in the *fakA* mutant (27). In agreement with previous research, we observed a significant increase in cellular free fatty acids in the *fakA* mutant compared to wild type (Figure 1A) at 6 hours. However, the cellular fatty acid levels were slightly, but significantly, decreased at 3 hours. The identity of the individual fatty acids was also determined, and we observed differences in several fatty acid species between wildtype and *fakA* mutant after 3 hours of growth (Figure S2A) and 6 hours of growth (Figure S2B). Specifically, we found a significant ($p<0.05$) increase in the proportion of 15:0, 17:0, 19:0, and 20:0 in the *fakA* mutant during late exponential (6 hours) growth phase. We reasoned that an accumulation of fatty acids in the cell could lead to release of fatty acids into the supernatant. We observed an increased abundance of supernatant fatty acids in both strains over time, which was enhanced in the *fakA* mutant (Figure 1B). These data demonstrate that the *fakA* mutant accumulates less fatty acids during early exponential phase (3 hours) of growth but accumulates more fatty acids during late exponential phase (6 hours) of growth compared to wildtype. It also identifies that the *fakA* mutant possesses altered fatty acid pools compared to the wild-type strain.

Lipid profile for wild type and *fakA* mutant in TSB. An in-depth analysis of how FakA affects the composition of the lipid membrane of *S. aureus* has not been undertaken. To do this, we performed a comprehensive analysis of the membrane lipids of *fakA* mutant compared to that of wild type when grown in TSB. Lipids were extracted using a modified Bligh and Dryer liquid-

liquid lipid extraction protocol (30). Since lipid ratios are known to vary by growth phase (31, 32), we examined cells during exponential phase (5 hours) and stationary phase (24 hours). As expected, PG and LPG were the primary lipids in both cells (Figure 2A and 2B). We observed little difference between the major lipid species between the two strains, with only a modest significant increase in PG and corresponding decrease in CL in the *fakA* mutant during exponential phase of growth (Figure 2A). Since LPG and CL are synthesized from PG, the lack of major differences was not unexpected as FakA is important for insertion of exogenous fatty acids as phospholipid acyl side chains and not, as far as we know, the activity of the enzymes responsible for lipid species generation. Considering this, we determined the total carbon and saturations of the lipid acyl side chains for PG and LPG in the wildtype and *fakA* mutant. During growth in TSB, lipids containing an unsaturated acyl-chain were near absent at either phase of growth in both strains (Figure 2C and 2D). We did identify significant changes in the lipid profiles between the two strains with the *fakA* mutant tending to contain a higher abundance of longer acyl sides chains, predominantly 35:0, than the parent strain.

Since the data in Figure 2C and 2D represents the total carbon length of both acyl side chains, we performed product ion analysis on pooled samples to determine the most abundant acyl side chain pairings that comprise each lipid (Table S1). This analysis revealed that both wildtype and the *fakA* mutant use 15:0 as one acyl sidechain, as expected. The second acyl moiety was the same for each lipid species between the two strains, i.e. 35:0 possessed a 15:0 and 20:0 fatty acid. Thus, despite using the same fatty acids for membrane generation, the mutant possesses a higher percentage of longer acyl-chain containing lipids.

Lipid profile of wild type and *fakA* mutant in presence of exogenous fatty acid. *S. aureus* is unable to endogenously synthesize unsaturated fatty acids but can incorporate them from the

environment through FakA. This allows us to use exogenously added fatty acids to track exogenous fatty acid utilization and observe where exoFAs are incorporated. Using this approach, we determine the lipid composition of both wildtype and a *fakA* mutant when grown in the presence of oleic acid (18:1), which was chosen due its relatively low toxicity (Figure S3) (28). Previously, we demonstrated that the addition of 0.001% (~31 μM) oleic acid elicits a transcriptional response in *S. aureus* (25); therefore, we determined the lipid profiles in TSB supplemented with 0.001% oleic acid. We observed little if any incorporation of oleic acid into PG and LPG when grown at this concentration (Figure 3A and 3C). Indeed, the lipid profile of wildtype and *fakA* mutant grown with added 0.001% oleic acid were indistinguishable from growth in TSB alone (Figure 2). In agreement with this, we used fatty acid methyl ester (FAME) analysis followed by gas chromatography to examine total fatty acid content of the cells and found little oleic acid (18:1) associated with the cells grown in TSB + 0.001% oleic acid (Table S2). Thus, while *S. aureus* responds transcriptionally to 0.001% additional oleic acid, this concentration was too low to affect incorporation.

Next, we increased the oleic acid concentration to 0.01% oleic acid (~314μM). At this concentration, the wild-type strain readily used the oleic acid and was observed as the appearance of a single unsaturated fatty acid chain primarily in 32:1, 33:1, 34:1, and 35:1 lipids (Figure 3B and 3D). We had predicted that oleic acid (18:1) would be found primarily paired with 15:0, the most common fatty acid lipid side chain in *S. aureus*. While we did readily detect 33:1, the most abundant lipid was 35:1 and composed >30% of total lipid species. As expected, there was no unsaturated fatty acid in the lipids isolated from the *fakA* mutant. To confirm that the absence of oleic acid in *fakA* mutant lipids is not due to oleic acid not associating with the cell, we performed FAME followed by gas chromatography analysis on the same extracts used for lipid analysis. Our

FAME analysis revealed that in TSB, the wildtype and *fakA* mutant have similar total fatty acids profiles, with increased 20:0 in the *fakA* mutant (Figure 4A). When grown with the additional 0.01% oleic acid, this fatty acid was readily detectable from both strains (Figure 4B and Table S2). FAME identifies all fatty acids, both free and lipid associated. Since oleic acid was identified by FAME but was not found as a component of the *fakA* lipids, we can conclude that oleic acid associates with the cells but cannot be incorporated into the *fakA* mutant. Thus, the lack of oleic acid in mutant membranes is due to a lack of incorporation and not because oleic cannot interact with or enter the cell.

Our lipid profiling indicated that wild-type cells can pair oleic acid with more than one fatty acid to produce a lipid. Moreover, we had expected 33:1 to be the most prevalent lipid species by pairing oleic acid with 15:0. We again used product ion analysis to determine the fatty acid pairing in each lipid (Table S1). It was expected that the fatty acid paired with oleic acid would be a saturated fatty acid and that this fatty acid would be equivalent to total lipid carbon length minus the oleic acid. This prediction was true for 32:1 (14:0 and 18:1) and 33:1 (15:0 and 18:1). Considering 18:1 was the added fatty acid, we anticipated 35:1 to be comprised of 17:0 and 18:1 fatty acids. This was not the case as the major 35:1 fatty acid pair consisted of 15:0 and 20:1. The inclusion of 20:1 was also the fatty acid associated in the lower abundant lipid 34:1.

While *S. aureus* membranes comprise both straight-chain fatty acids (SCFAs) and branched-chain fatty acids (BCFAs), it relies on BCFAs to modulate the rigidity of its lipid membrane (23). BCFAs in *S. aureus* are comprised of odd numbered iso and anteiso fatty acids and the proportions of BCFAs and SCFAs are highly dependent on the growth environment (21). We analyzed our FAME data to determine if the absence of *fakA* or the addition of oleic acid impacts BCFA or SCFA preference (Table S2). In TSB alone, wildtype and the *fakA* mutant have similar ratios of

anteiso/iso fatty acids (~1.5) and BCFA/SCFA (1.65 for wildtype and 1.48 for *fakA* mutant). Not surprising considering our other analysis, when grown in TSB+0.001% oleic acid, the fatty acid profile of both wildtype and *fakA* mutant was nearly identical to growth in TSB. By contrast, growth in TSB+0.01% oleic acid resulted in accumulation of oleic acid in both wildtype and *fakA* mutant bacteria. When comparing the BCFA/SCFA ratio under this condition, we observed a dramatic shift, most likely due to the added SCFA oleic acid. For example, wild-type cells grown in TSB contain ~38% SCFA while growth in 0.01% oleic acid led to the cells altering the fatty acid pools to ~78% SCFA. A similar shift (40% to 84%) was also seen in the *fakA* mutant. As noted in previous studies (33), the wild-type *S. aureus* unsaturated fatty acid pool was comprised of both C18:1 and C20:1. This data, along with our lipid and product-ion data, indicates that wild-type *S. aureus* elongates oleic acid (C18:1) to C20:1. This is not observed in the *fakA* mutant, as the majority of oleic acid remained oleic acid. In conclusion, the fatty acid composition of the membrane is dramatically altered in the presence of incorporation-level oleic acid seen in wildtype as the incorporation of oleic acid into PG, LPG and CL.

Membrane function is affected by the inability to utilize exoFAs. The membrane lies at the interface of cellular processes and the external environment. We have now shown that *fakA* influences membrane composition. We previously reported that the *fakA* mutant produces decreased pigment (28), which is associated with membrane fluidity (34-36). Also, our previous metabolomics study found that the *fakA* mutant has a more reduced cellular environment (27). The electron transport chain is embedded in the phospholipid membrane, suggesting that fatty acid accumulation and the composition of the membrane may affect respiration. Finally, membrane potential is indicative of metabolic state and membrane function. Therefore, we wanted to

224 determine the role FakA and exoFAs play in membrane fluidity, permeability, membrane potential,
225 and respiratory chain activity.

226 First, membrane fluidity was determined using the fluorescent probe 1,6-diphenyl-1,3,5-
227 hexatriene (DPH) (23, 34) in wild type and *fakA* mutant grown to exponential phase (5 hours) in
228 TSB with and without incorporation level oleic acid (0.01%). While it did not reach significance
229 (p=0.07), the *fakA* mutant had decreased membrane fluidity compared to wild type (Figure 5A).
230 The Crt-derived pigment staphyloxanthin is known to affect membrane fluidity (37) and *fakA*
231 mutants produce less pigment (37). To remove this complication, we tested a *crtM* mutant with
232 and without *fakA*. We observed that a *crtM* mutant has more membrane fluidity than its isogenic
233 parents, both in the case of wild type and *fakA*. Interestingly, a *fakA crtM* double mutant has
234 significantly decreased membrane fluidity compared to that of the *crtM* mutant. The addition of
235 0.01% oleic acid decreased membrane fluidity for both wild type and *fakA* mutant. This was not
236 due to incorporation as part of phospholipids since the wildtype and *fakA* mutants were equivalent.
237 For reasons that are not clear, adding oleic acid to *crtM* mutants had no effect on membrane fluidity
238 (compare *crtM* +/- oleic acid) and, again, we observed lower membrane fluidity in the *fakA crtM*
239 mutant compared to *crtM* alone. Thus, we identified that the absence of FakA affects membrane
240 fluidity and this is not due to the altered pigment levels in the mutant.

241 We next assessed whether the absence of FakA altered membrane integrity using propidium iodide
242 (P.I.) as an indicator since this stain cannot diffuse into cells unless membranes are compromised.
243 Cells were grown in TSB and membrane integrity was determined when grown in the presence
244 and absence of 0.01% oleic acid. When grown in TSB alone until mid-exponential phase, the
245 wildtype and *fakA* mutant had approximately 3% and 1.1% P.I. positive cells, respectively (Figure
246 5B). However, when cells grown in the presence of 0.01% oleic acid, 16.4% of wildtype cells were

P.I. positive compared to that of 2.8% for the *fakA* mutant. Thus, when grown in TSB, the *fakA* mutant has less permeable membranes whose permeability is less affected by the presence of oleic acid than the wild-type strain.

Membrane potential is important for driving ATP production and transporting ions and metabolites into and out of the cell. We determined the membrane potential ($\Delta\Psi$) of wild-type and *fakA* mutant *S. aureus* using the fluorescent reporter 3,3′-diethyloxacarbocyanine iodide ($DiOC_2(3)$) (38, 39). Wildtype and *fakA* had similar membrane potentials when grown in TSB alone (Figure 5C). When grown in the presence of 0.01% oleic acid, both strains had decreased membrane potentials compared to that when grown in TSB alone, but this was enhanced in the *fakA* mutant with a 40% reduction compared to a 20% reduced potential in WT. Thus, under these conditions, oleic acid decreases membrane potential and this may be enhanced in a *fakA* mutant.

Electron transport chain activity was measured using the fluorescent reporter 5-cyano-2,3-ditolyl tetrazolium chloride (CTC) (39). This reporter is reduced by respiratory dehydrogenases and is thus indicative of cellular respiration. In TSB alone, the *fakA* mutant had significantly more respiratory activity compared to that of wildtype (Figure 5D). However, both wildtype and *fakA* mutant display decreased respiratory activity in the presence of incorporation-level oleic acid, which correlates with reduced growth (Figure S3). Overall, these studies demonstrate that the *fakA* mutant displays phenotypes that are associated with membrane changes.

Lipid profile is altered when grown in the presence of mouse skin homogenate. The most common infection site of *S. aureus* is the skin, which contains high levels of various fatty acids and lipids (40). These molecules have antimicrobial properties and limit the growth of certain bacteria. It is unknown if *S. aureus* can utilize fatty acids from mouse skin, though it will harvest fatty acids from other host molecules such as low-density lipoprotein (41). To gain insight into

this, we determined 1) if *S. aureus* alters its lipids in response to mouse skin, and 2) if *S. aureus* incorporates host fatty acids. To this end, we grew wild-type and *fakA* mutant *S. aureus* in a combination of 75% mouse skin homogenate and 25% TSB. This ratio was chosen based on relatively high bacterial growth (OD_{600} 3.5-4.5) to allow for quality extraction of bacterial lipids. After 24 hours of growth in 75% mouse skin homogenate, cells were isolated, lipids were extracted, and analyzed via LC/MS/MS. To ensure that we did not collect mouse skin lipids without bacterial cells, one sample of 75% mouse skin homogenate and 25% TSB without bacterial cells was treated identically to our bacterial cells we extracted. This sample without bacteria was also analyzed via LC/MS/MS and we found only trace amounts of lipids (Figure S4), demonstrating that our data represents lipids isolated from *S. aureus* and not contaminates from the mouse skin. Under this growth condition, we observed equal levels of PG and LPG in the wild-type strain. Unlike in TSB, we saw a pronounced difference in the *fakA* mutant compared to wildtype. In this case, the *fakA* mutant resembled membranes of cells grown in TSB alone with PG being the most abundant, followed by LPG, and CL being the least abundant lipid. The most abundant saturated PG species was 33:0 and 35:0 in wildtype while the *fakA* mutant had a relatively even distribution of 32:0, 34:0, and 35:0. Using the natural unsaturated fatty acids found in mouse skin as a marker of host fatty acid utilizations, we observed considerable incorporation of unsaturated fatty acids as a component of the wild-type cell lipids (Figure 6B-D). The unsaturated PG species 33:1, 34:1, 35:1 and 36:1 were all found in *S. aureus* grown in mouse skin homogenate. Similar trends were observed for LPG and CL species. We did not identify lipids containing more than one fatty acid unsaturation. As expected, we did not find unsaturated fatty acids in the lipids of the *fakA* mutant. In conclusion, we show that *S. aureus* can utilize unsaturated fatty acids found in mouse skin homogenate for lipid synthesis.

Discussion

The exogenous fatty acid utilization system of *S. aureus* has recently emerged as a new metabolic pathway and is made up of at least the fatty acid kinase FakA and the fatty acid binding partner proteins FakB1 and FakB2 (18, 20). Despite the characterization of this system, how inactivation of this pathway (via deletion of *fakA*) affects the composition of the phospholipid membrane has been unknown. *S. aureus* is routinely cultivated in TSB which is abundant in carbohydrates, protein, and fatty acids, primarily palmitic acid (C16:0) and stearic acid (C18:0). Not surprisingly, based on a previous report, we identified an accumulation of fatty acids in a *fakA* mutant under our growth conditions. However, our studies revealed that this changes over the course of growth and identifies that not only do the *fakA* mutant cells accumulate fatty acids, but that fatty acids are released into the media where they also increase in abundance. It is unknown whether this accumulation of fatty acids in the extracellular growth environment is an intentional process (i.e. release of fatty acids from the cell), due to cell death and turnover, or are actively released by a efflux system that has been proposed (29). Since only free fatty acids are identified in this experiment, the fatty acids found in the supernatant are likely not part of extracellular membrane vesicles produced by *S. aureus*. The consequence of altered fatty acid metabolism in the *fakA* mutant is not a change in the ratio of primary lipid species, but a reorganization of the fatty acid phospholipid side chains. Moreover, we demonstrate that the addition of excess 18:1 fatty acid leads to its incorporation into wild-type cells, but also a change in the fatty acid pools in both wildtype and *fakA* mutant.

S. aureus is known to produce primarily three phospholipids (8, 42-44). Phosphatidylglycerol (PG) is the primary phospholipid and is the precursor for the generation of additional phospholipids. Lysl-PG (or LPG) is produced by MprF and while *S. aureus* has two cardiolipin synthases,

316 cardiolipin is the least abundant species. As expected, our results demonstrated that both wild-type
317 and *fakA* mutant membranes primarily contained PG and LPG. The amount of CL can vary by
318 strain and condition, and we detected only 4.5% of total phospholipids as cardiolipin in our
319 USA300 *S. aureus* strain at either exponential or stationary phase of growth showing that LAC
320 derivatives grown under our conditions produce little CL.

321 *S. aureus* generally prefers endogenously produced 15:0 in the sn2 position of the phospholipids
322 and will insert either a second endogenous fatty acid or exoFA in the sn1 position. Our product
323 ion analysis of the wild-type and *fakA* mutant phospholipids most often contained a 15:0 fatty acid.
324 However, the *fakA* mutant paired this 15:0 more frequently with longer chain fatty acids (Figure
325 2) than the parent strain. Phospholipids of lower total carbon abundance (i.e. 30:0, 31:0, 32:0, and
326 33:0) were more abundant in wildtype compared to that of *fakA* mutant. These phospholipids all
327 contained C15:0 in one sn position, with the other acyl chain being C15:0, C16:0, C17:0, and
328 C18:0 in phospholipids 30:0, 31:0, 32:0 and 33:0, respectively. The most abundant phospholipids
329 observed in wildtype were 32:0 and 33:0. In contrast, the *fakA* mutant tended to have larger fatty
330 acids as part of phospholipids, shifting to 35:0 in both PG and LPG due to the insertion of C20:0
331 alongside C15:0. This was also reflected in the free fatty acid pools in the *fakA* mutant (Figure S2)
332 showing that this mutant possesses and uses a greater abundance of longer fatty acids such as 19:0
333 and 20:0. However, the presence of exogenous oleic acid altered the normal relationship of use of
334 15:0 alongside a varying-length second fatty acid. In this case, the wild-type generated lipids with
335 18:1 oleic acid in combination with not only 15:0, but also commonly 14:0. One observation made
336 from this study, and in agreement with Parsons et al (33) in strain RN4220, is the abundance of
337 fatty acid C20:1 in wildtype *S. aureus*. Since oleic acid (C18:1) was the exogenous fatty acid added
338 to the media, this demonstrates that *S. aureus* can elongate exoFAs. This was a frequent event

since 35:1 composed of 15:0 and 20:1 was the most abundant lipid species identified in wild type when grown in the presence of oleic acid (Table S1 and Fig. 3). Our FAME analysis confirmed that the lack of incorporation of 18:1 into the *fakA* mutant is not due to the inability to associate with the cells and is a result of the inability of the *fakA* mutant to phosphorylate the fatty acid, as expected. The presence of 20:1 has been observed previously and while the exact mechanism behind exoFA elongation has not been elucidated, it has been proposed to occur through FabF, part of the fatty acid biosynthesis pathway (45). However, our observation that there was no 20:1 fatty acid found in the *fakA* mutant, demonstrates that elongation of exoFAs requires FakA and that only phosphorylated fatty acids can be elongated by *S. aureus*.

In previous studies, we identified that oleic acid can inhibit the Sae two-component system when added exogenously to the media at 0.001% (25). This was later confirmed by another group (26). Considering this transcriptional response, we anticipated that this concentration would yield membranes containing oleic acid. However, oleic acid-containing phospholipids were not detected when *S. aureus* was grown in the presence of 0.001% (~31μM) oleic acid. When the concentration of oleic acid was increased ten-fold to 0.01% (~314μM), we observed incorporation of oleic acid into lipids. Thus, there is an apparent concentration-dependent incorporation of exogenous unsaturated fatty acids by *S. aureus*. Moreover, this data revealed that *S. aureus* can sense and respond transcriptionally to levels of fatty acids that are lower than those used for membrane synthesis, further supporting fatty acids as a potent signaling molecule in *S. aureus*.

The membrane is a dynamic structure that dictates multiple functions of the cell. We identified functional changes between wild-type and *fakA* mutant *S. aureus*. In TSB alone, the *fakA* mutant has more rigid membranes regardless of pigment production. Since pigment impacts membrane fluidity and the *fakA* mutant produces less pigment, this could confound membrane fluidity

362 experiments in this strain. Our data confirms that pigment does impact membrane fluidity (Fig. 5),
363 but also demonstrates that there is a FakA-dependent component. This could possibly be due to
364 increases in the acyl-chain length of the phospholipids (Figure 2C) as longer acyl-chains result in
365 a more rigid membrane. Additionally, a slight decrease in BCFA/SCFA ratios in the *fakA* mutant
366 (Table S2) could increase rigidity. To our surprise, addition of 0.01% oleic acid decreased
367 membrane fluidity of both wildtype and *fakA* mutant. While the unsaturated fatty acid linoleic acid
368 (C18:2) has been shown to increase membrane fluidity (46), our data clearly demonstrates that
369 growth in the presence of oleic acid does not result in similar membrane fluidity. There may be
370 two explanations for this possible result. First, this may be due to the difference in structure of the
371 fatty acids. The presence of two unsaturations in linoleic acid may be more disruptive to fluidity
372 compared to that of oleic acid. Secondly, the addition of 0.01% oleic acid dramatically decreases
373 the BCFA/SCFA ratio in both wildtype and *fakA* mutant. To this end, wild-type cells contained
374 38% and >75% SCFAs when grown in TSB without or with 0.01% oleic acid, respectively.
375 SCFAs, like oleic acid, are known to affect membrane fluidity and our data are consistent with the
376 increased abundance of SCFAs when grown in the presence of oleic acid decreasing membrane
377 fluidity. It appears that oleic acid impacts membrane fluidity without the requirement of being
378 incorporated and this is influenced by the presence of the pigment staphyloxanthin. Notably,
379 previous work suggests that pigment levels are not influenced by fatty acid incorporation (47).
380 Dissecting this relationship between fatty acid addition, fatty acid utilization, and *S. aureus*
381 pigmentation will be the focus of future studies.

382 We have established that the *fakA* mutant has altered metabolism (27). Since the electron transport
383 chain is embedded in the phospholipid membrane, we sought to determine whether the changes in
384 membrane composition in the *fakA* mutant and the presence of 0.01% oleic acid altered cellular

385 respiration. The *fakA* mutant had more respiratory activity than wildtype in TSB alone (Figure
386 5D). This agrees with our metabolic study showing the *fakA* mutant had an increase in
387 NAD+/NADH and NADP+/NADPH levels at the same phase of growth. Growth in TSB+0.01%
388 oleic acid resulted in decreased respiration in both wildtype and the *fakA* mutant. While the
389 increased respiration of the *fakA* mutant in TSB didn't affect membrane potential, growth in
390 TSB+0.01% oleic acid depolarized both the wildtype and *fakA* mutant; however, the *fakA* mutant
391 was more greatly affected (Fig. 5C). Previous studies indicated that palmitoleic acid (C16:1), and
392 not oleic acid (C18:1), depolarized membranes (45). It should be noted that we used approximately
393 three times the concentration of oleic acid as the study mentioned and can likely account for the
394 differences between experiments. Additionally, the study mentioned above was published prior to
395 the identification of FakA and therefore, how incorporation vs free fatty acid exposure could not
396 be tested. Thus, our data indicates that oleic acid will decrease respiration and depolarize
397 membranes at 0.01% (314 μM) regardless of being incorporated into phospholipids. Why the *fakA*
398 mutant has more respiratory activity in TSB is unknown; however, this observation occurs at a
399 point where we identified enhanced growth in the *fakA* mutant during the switch between glucose
400 and acetate/amino acid utilization (27). Thus, it may be not surprising to see increased respiratory
401 activity during periods of enhanced growth. Why FakA influences metabolism and has not been
402 completely elucidated. This could be due to changes in the membrane that may influence nutrient
403 diffusion or transport. Another possibility is the result of the accumulation of fatty acids, which
404 could have different activities or impact levels based on saturation. A recent study indicated that
405 inactivation of type II NADH dehydrogenases, (Ndh-2s) particularly NdhC, results in fatty acid
406 accumulation and regulation of the SaeRS two-component system (48). Ndh-2s do not pump ions
407 across the membrane, thus playing an indirect role in membrane potential. In *E. coli*, Ndh-2s are

associated with aerobic respiration while Ndh-1s are associated with anaerobic respiration (49). Since the *fakA* mutant possesses an aeration-dependent growth enhancement and has increased respiratory activity without a significant increase in membrane potential, we predict that the Ndh-2 are playing a pivotal role in altering metabolism when fatty acids are accumulated within the cell or in the presence of exogenous fatty acids. Studies testing how different types of exogenous fatty acids affect respiration through Ndh-2s, as well as other members of the respiratory chain, will help us understand the mechanism by which fatty acids are affecting bacterial physiology. It is clear that the inability of *S. aureus* to use fatty acids and/or exposure to exogenous fatty acids impacts physiology. This has been seen by us and others as changes in the glucose, acetate, amino acid metabolism, and energy or redox homeostasis that apparently involves at some level NADH dehydrogenases and regulatory proteins such as CcpA, as well as transcriptional response in arginine deiminase and urease (27, 28, 45, 48, 50, 51). It is also possible that *S. aureus* identifies unsaturated fatty acids as a stress as we previously saw that enhanced resistance to unsaturated fatty acids in a *fakA* mutant requires the alternative sigma factor σ^B (28). Future studies will be needed to determine the specific mechanism by which fatty acid addition modulate metabolism in *S. aureus* and whether this is a general fatty acid response or is restricted to certain fatty acids types.

We wanted to expand our observations to more closely mimic what the bacteria may encounter during infection. Since *S. aureus* commonly causes infections in the skin, we wanted to determine if *S. aureus* can actively scavenge unsaturated fatty acids for phospholipid synthesis from host tissue. To do this, we homogenized mouse skin and grew wild-type and *fakA* mutant *S. aureus* in 75% mouse skin homogenate supplemented with 25% TSB. While *S. aureus* can grow relatively well in 100% mouse skin homogenate, we added 25% TSB to ensure high bacterial growth. We

confirmed that *S. aureus* can scavenge exogenous fatty acids when grown in mouse skin homogenate. We did observe lipidome changes in wildtype *S. aureus* when grown in mouse skin compared to that of TSB+0.01% oleic acid. For example, growth in mouse skin resulted in wildtype *S. aureus* to have relatively similar levels of PG33:0, PG33:1, PG35:0, and PG35:1. This differs from growth in TSB+0.01% oleic acid, where PG35:1 clearly became the most abundant phospholipid. While other studies have found that *S. aureus* can utilize fatty acids from host source, specifically low-density lipoprotein and pig liver homogenate (41, 52), none have used homogenized skin as a medium. Given the propensity of *S. aureus* to commonly infect the skin, our data provides a framework for future studies utilizing skin as a source of fatty acids and how bacterial phospholipid membranes adapt to skin tissue. How *S. aureus* is scavenging fatty acids from mouse skin and whether they are derived from free fatty acids, lipids, or LDL is one component of ongoing studies.

The exoFA utilization pathway of FakB1, FakB2, and FakA is newly described (18, 24). Despite being necessary for the incorporation of exoFAs into the membrane, a detailed analysis of how this system alters membrane composition has not been performed. Not surprisingly, our results show no change in the PG:LPG:CL ratio by the absence of FakA, but there was a reorganization of the fatty acids side chains, e.g. change in fatty acid length preference, of *S. aureus* phospholipids in the absence of FakA. These studies provide key details on how membrane composition changes in response to exoFAs regardless if they are used for phospholipid synthesis. Furthermore, this work expands our knowledge on how the activity of FakA influences *S. aureus* physiology.

Materials and Methods

Bacterial strains, plasmids, and growth conditions. Bacterial strains and plasmids used in this study are listed in Table 1. *S. aureus* was grown in tryptic soy broth (TSB) or tryptic soy agar

supplemented with chloramphenicol (10 μg mL^{-1}) or erythromycin (5 μg mL^{-1}) when necessary. *S. aureus* cultures were then inoculated at a 1:10 media to flask volume ratio at an initial optical density at 600 nm of 0.1 in TSB and grown at 37ºC with shaking at 250 rpm. TSB was supplemented with oleic acid (Alfa Aesar) by adding indicated percent v/v oleic acid to media and vortexed vigorously before aliquoting into flasks.

Fatty acid analysis. Cell pellets and supernatants were flash frozen in liquid nitrogen and stored at -80ºC until processed. The cell pellets were washed three times with 1 mL of 40 mM ammonium formate in water. The washed pellets were re-suspended in 50 μL of 5 mM ammonium acetate and homogenized three times for 30 s with a BeadBeater with 15-min rests on ice in between. Protein concentration of the homogenates were measured, and each sample was normalized to 500 μg mL^{-1} and aliquoted at 25 μL for extraction. The supernatants were not normalized and aliquoted at 125 μL for extraction. All samples were extracted by protein precipitation with 1 mL of 80%/20% methanol/water for 20 min at 4°C. The samples were centrifuged at 20,000 x *g* for 10 minutes at 4°C. 1 mL of supernatant was collected and dried down under nitrogen gas at 30°C. The samples were reconstituted at 25 μL of 80:20 acetonitrile/5 mM ammonium acetate in water. Each sample was spiked with 1 μL of fatty acid stable isotope standards.

Analysis of the free fatty acids was performed on a Thermo Q-Exactive Oribtrap mass spectrometer with Dionex UHPLC and autosampler. All samples were analyzed in negative heated electrospray ionization in data dependent MS/MS with a mass resolution of 70,000 in Full MS and 17,500 at *m/z* 200 in data dependent MS/MS. Separation was achieved on an Acquity UPLC HSS T3 2.1 x 150 mm, 1.8 μm column with mobile phase A as 1 mM ammonium acetate and mobile phase B as 0.1% acetic acid in acetonitrile. The flow rate was 500 μL min^{-1} with a column

476 temperature of 30°C. Injection volume was 4 µL. Peak areas were integrated for each analyte and
477 internal standards using Xcalibur.

478 **ESI-MS/MS lipid profiling.** An automated electrospray ionization-tandem mass spectrometry
479 approach was used, and data acquisition and analysis and acyl group identification were carried
480 out as described previously (53) with modifications. Each sample was dissolved in 1 mL
481 chloroform and an aliquot of 2 to 39 µL of extract was used.

482 For analysis of PG, PA, monohexDAG, and dihexDAG, phospholipid and galactolipid internal
483 standards, obtained and quantified as previously described (54), were added in the amounts
484 indicated in Narayanan et al (55) except for: phosphatidylinositol (PI) (16:0/18:0) (0.28 nmol), PI
485 (18:0/18:0) (0.11 nmol), digalactosyldiacylglcyerol (DGDG) (18:0/16:0) (0.44 nmol),
486 DGDG(18:0/18:0) (1.48 nmol), monogalactosyldiacylglycerol (18:0/16:0) (1.67 nmol),
487 MGDG(18:0/18:0) (1.41 nmol), and cardiolipin (CL) (14:0/14:0/14:0/14:0) (0.015 nmol). The
488 sample and internal standard mixture was combined with solvents, such that the ratio of
489 chloroform/methanol/300 mM ammonium acetate in water was 300/665/35, and the final volume
490 was 1.4 mL. Analysis of PG, PA, monohexDAG, and dihexDAG was performed on unfractionated
491 lipid extracts introduced by continuous infusion into the ESI source on a triple quadrupole MS/MS
492 (API 4000, Applied Biosystems, Foster City, CA). Data were collected and analyzed as previously
493 described for analysis of PG, PA, monogalactosyldiacylglycerol (monohexDAG), and
494 digalactosyldiacylglycerol (dihexDAG) (55).

495 For CL and LPG analysis, phospholipid standards were added one-fifth of the amounts indicated
496 above. CL and LPG were analyzed on a triple quadrupole MS/MS (Xevo TQS, Waters Corp.,
497 Milford, MA). Samples were introduced to the Xevo TQS using a Waters 2777 Sample Manager
498 autosampler. Lipid species were detected with the following scans: LPG $[M-H]^-$ in negative ion

mode with Precursor 145.0; cardiolipin in negative ion mode with Precursor 153.0. The scan speed was 50 or 100 u per sec^{-1}. The Xevo TQS in negative ion mode has capillary, 2.8 kV, cone voltage, 40 V, source temperature, 150°C, desolvation temperature, 120°C, collision gas, 0.14 mL/min, nebulizer gas flow 7 bar for CL and LPG. Collision energies on the Xevo TQS, with argon in the collision cell, were -75 V for CL, and -35 V for LPG.

Data processing was similar to that previously, including background subtraction, smoothing, integration of spectral peaks, isotopic deconvolution, correction for chemical or instrumental noise, and quantification (56, 57). Internal standards of the same class were used for PA, PG, and cardiolipin. Lysyl PG was quantified against the PG(40:0) in negative Precursor mode, monohex and dihexDAG were quantified against PG(40:0) in positive NL mode. Finally, the data were corrected for the fraction of the sample analyzed and normalized to signal per CFU to produce data in the units nmol/1e10 CFU.

Product ion analyses were performed on pooled replicates of the treatments on the 4000 QTrap mass spectrometer in enhanced product ion mode. Aliquots of 11 to 14 uL were used. Collision energy was varied as needed for sufficient fragmentation, starting at -45 V. The curtain gas was 10 mL/min, CAD gas was medium, and the electrospray capillary voltage was -4500 V.

Membrane fluidity, integrity, potential, and ETC activity. Membrane fluidity for wildtype and *fakA* mutant strains were carried out as previously described (58). Membrane integrity was determined using propidium iodide (P.I.) as an indicator. Wildtype and *fakA* mutant bacteria were grown in TSB with or without 0.01% (314 μM) oleic acid for 5 hrs. 1.2 mL of culture spun down and resuspended in 600 μL PBS. The cells were then diluted to an OD_{600} = 0.25 in 500 μL in PBS. As a control, one sample was diluted to OD_{600} = 0.25 in 500 μL 70% ethanol. 1 μL of P.I. (50

mg/mL) was added to the cells and allowed to incubate at room temperature for 15 minutes. P.I. positive cells were determined using flow cytometry.

Membrane potential was determined using the *Bac*Light Bacterial Membrane Potential Kit (Molecular Probes, Invitrogen) (39). Wildtype and *fakA* mutant bacteria were grown for 5 hrs. Cultures were diluted to an OD_{600} = 0.1 in 1 mL PBS. As a negative control, 10 µL of 500 µM carbonyl cyanide *m*-chlorophenyl hydrazone (CCCP) was added to one sample and vortexed. 10 µL of 3mM $DiOC_2(3)$ was then added to all samples, excluding a no stain control, and vortexed. Samples were then allowed to incubate at room temperature for 30 minutes and analyzed via flow cytometry. The data is presented as the geometric mean ratio of red:green using TexasRed and FITC filters, respectively.

Electron transport chain activity (respiratory activity) was determined using the *Bac*Light RedoxSensor CTC Vitality Kit (Molecular Probes, Invitrogen) (39). Wildtype and *fakA* mutant bacteria were grown for 5 hrs. Cultures were diluted to and OD_{600} = 0.1 in 650 µL PBS. One sample was diluted in 70% ethanol as a negative control. 65 µL of 50 mM CTC was added to each sample, except for a no stain control. The samples were then incubated in the dark at 37˚C for 30 minutes and analyzed using a Tecan Spark 10M plate reader (Excitation 485+/-20nm and Emission 645+/-40nm).

Generation of mouse skin homogenates. These studies were conducted under an approved protocol by the Institutional Animal Care and Use Committee (IACUC) of the University of Kansas Medical Center. We used mice of the C57BL/6 background. Following sacrifice, mice were shaved and treated with Nair to remove remaining hair. Next, skin was removed and homogenized in PBS using Lysing Matrix H with a FastPrep-24 5G following manufacturer's setting. Homogenates were pooled and sequentially passed through 40 µm and 0.45 µm filters.

Table 1. List of stains used in this study.

Strain or plasmid	Relevant characteristics[a]	Reference
AH1263	USA300 CA-MRSA strain LAC without LAC-p03	(59)
JLB2	AH1263 Δ*fakA*	(24)
JLB112	AH1263 *crtM::*NΣ	(28)
JLB129	JLB2 *crtM::*NΣ	(28)
pJB165	*fakA* complement plasmid	(24)

[a] NΣ indicates mutations originating from the Nebraska Transposon Mutant Library

Acknowledgements

This research was supported by funding from the National Institute of Allergy and Infectious Diseases (NIAID) award R01AI121073 to JLB, and a pilot project grant through award P20GM112117. We would like to thank Miranda Ridder for the help in harvesting mouse skin for the mouse skin homogenate experiments. The lipid analyses described in this work were performed at the Kansas Lipidomics Research Center Analytical Laboratory and would not have been possible without Dr. Ruth Welti and Mary Roth. Instrument acquisition and lipidomics method development were supported by the National Science Foundation (including support from the Major Research Instrumentation program; current award DBI-1726527), K-IDeA Networks of Biomedical Research Excellence (INBRE) of National Institute of Health (P20GM103418), USDA National Institute of Food and Agriculture (Hatch/Multi-State project 1013013), and Kansas State University. We are grateful to Dr. Tim Garrett at the Southeast Center for Metabolomics the free fatty acid analysis done for this research (NIH grant #U24 DK097209).

559 Dr. Bose serves on the Scientific Advisory Board and is a consultant for Azitra, Inc. These
560 activities did not financially support and are unrelated to the current manuscript.

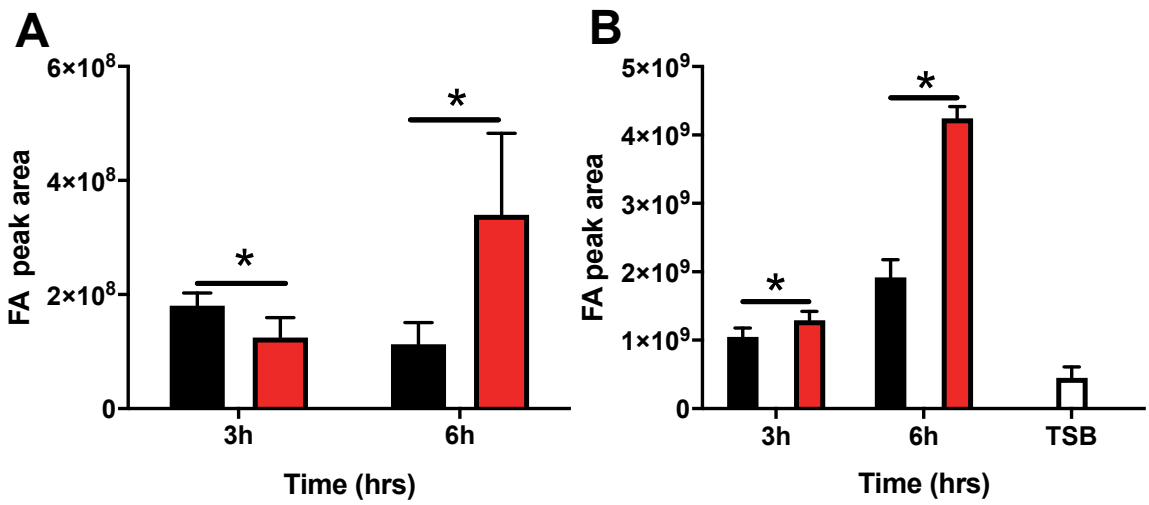

561

562 **Figure 1.** Cellular **(A)** and supernatant **(B)** free fatty acids (FA) of wildtype (black) and *fakA*
563 mutant (red) grown for three and six hours in TSB+14mM glucose. Empty bar is free fatty acids
564 from sterile TSB+14mM glucose. Data represents the mean (n=4) with standard deviation,
565 *$p<0.05$ by student t-test.

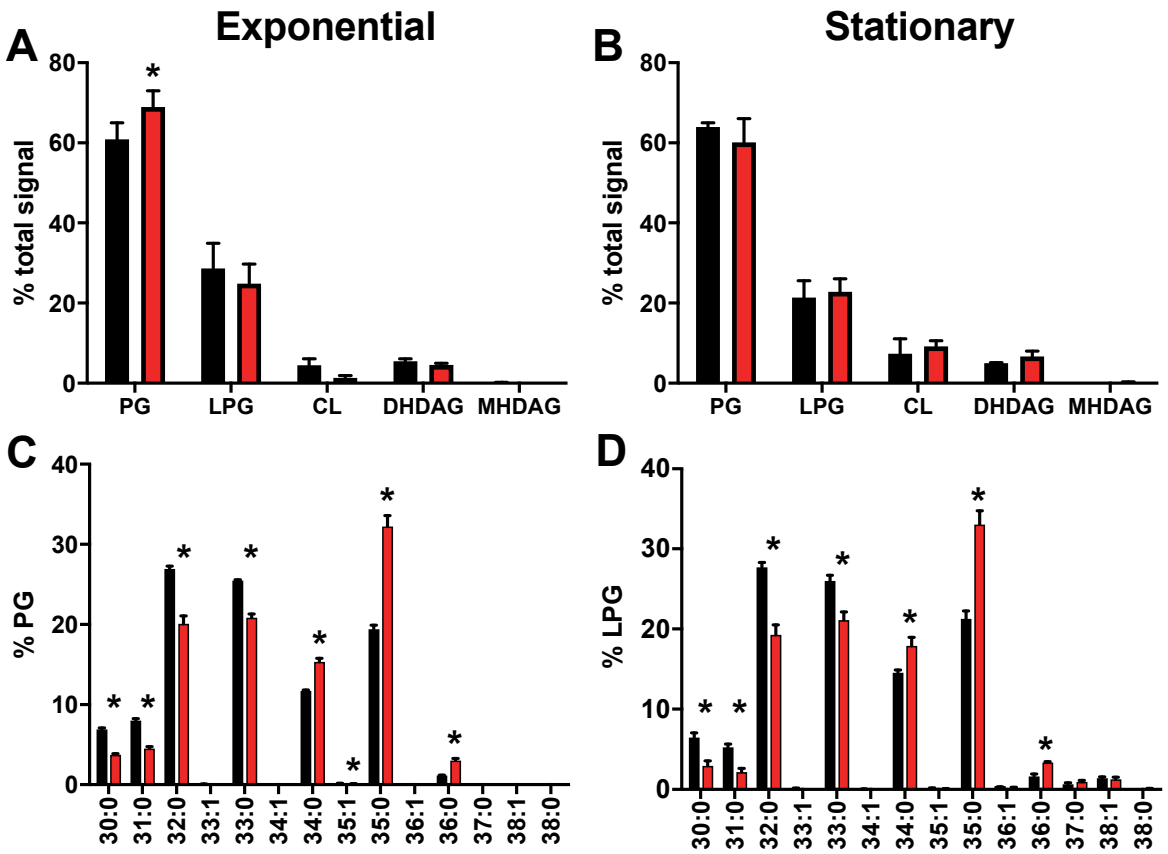

566

567 **Figure 2.** Lipid analysis for wildtype (black) and *fakA* mutant (red). % total signal for each lipid
568 class was determined at **(A)** exponential and **(B)** stationary phase of growth for
569 phosphatidylglycerol (PG), lysyl-PG (LPG), cardiolipin (CL), dihex-diacylglycerol (DHDAG),
570 and monohex-diacylglycerol (MHDAG). Individual **(C)** PG and **(D)** LPG species from cells in
571 exponential phase were determined and are presented as percent of the total PG or LPG signal.
572 Data represents the mean (n=4) with standard deviation, *$p<0.05$ by student t-test.

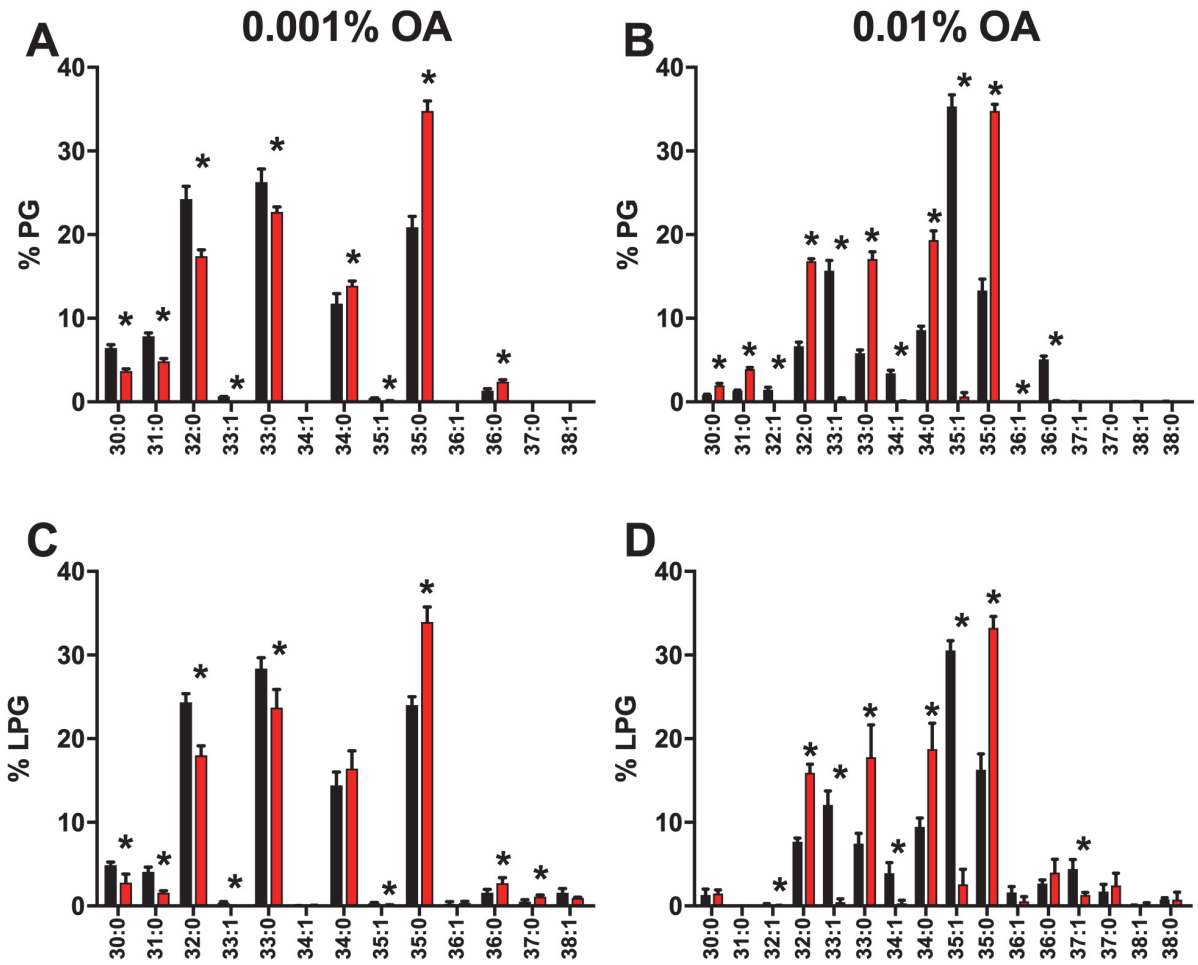

573

574 **Figure 3.** Lipid profile for wildtype (black) and *fakA* mutant (red) of PG **(A** and **B)** and LPG **(C**
575 and **D)** grown in TSB+0.001% oleic acid **(A** and **C)** or TSB+0.01% oleic acid **(B** and **D)**. Data
576 represents the mean (n=4) with standard deviation, *p<0.05 by student t-test.

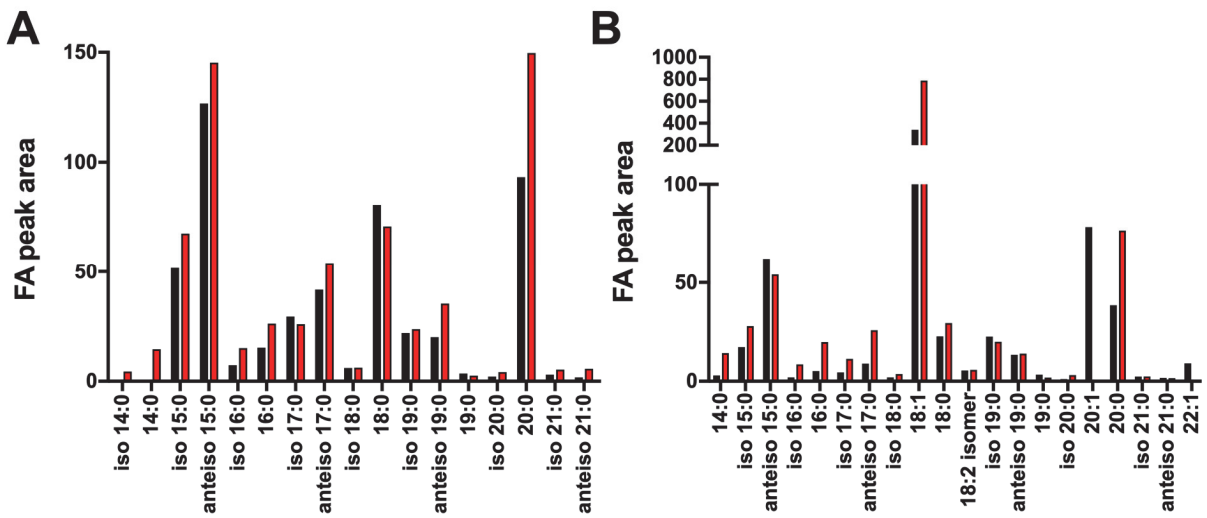

577

578 **Figure 4.** Fatty acid methyl esterase analysis of lipid extracts from wildtype (black) and *fakA*

579 mutant (red) grown in TSB **(A)** or TSB+0.01% oleic acid **(B)**. Data is from pooled replicates (n=4)

580 from each strain and growth environment.

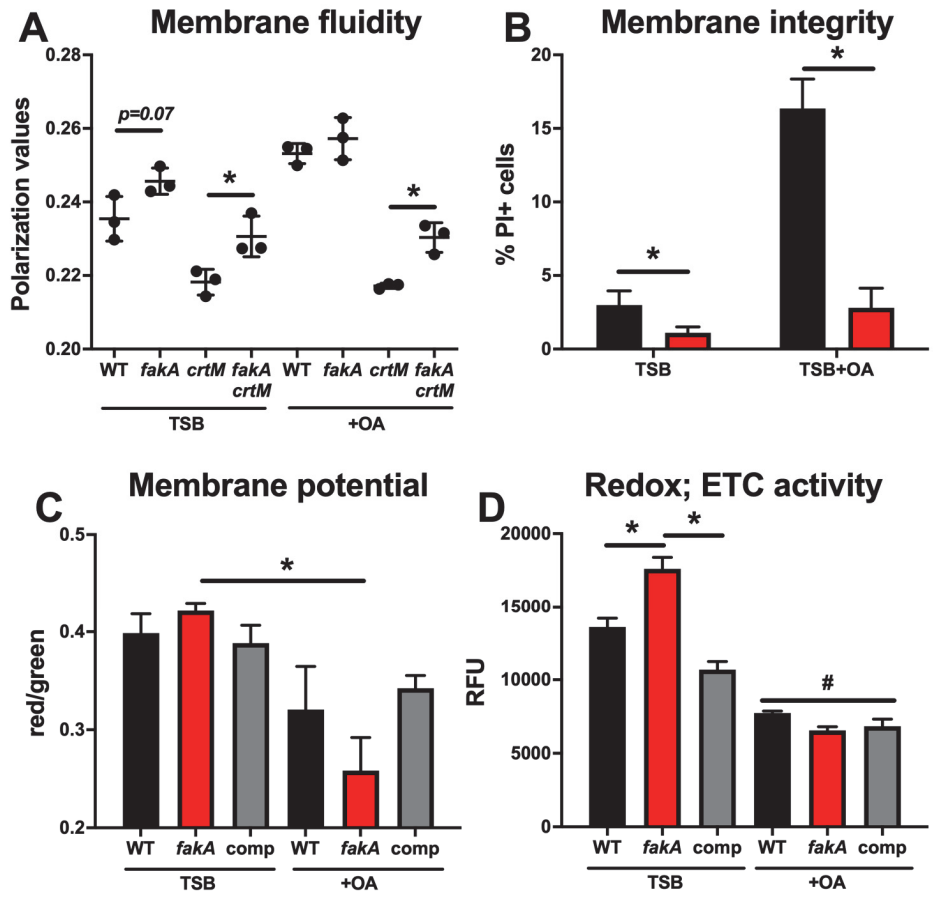

581

582 **Figure 5. (A)** Membrane fluidity in wildtype, *fakA* mutant, *crtM* mutant, and *fakA crtM* mutants
583 grown in presence (+OA) or absence (TSB) of 0.01% oleic acid. **(B)** Membrane integrity measured
584 using propidium iodide (P.I.) as an indicator for wildtype (black) and *fakA* mutant (red). **(C)**
585 Membrane potential was analyzed using $DiOC(3)_2$ staining of wildtype (black), *fakA* mutant (red),
586 and complemented *fakA* mutant (comp, grey). **(D)** Respiratory activity of wildtype (black), *fakA*
587 mutant (red), and complemented *fakA* mutant (comp, grey) as measured using CTC as an indicator.
588 Data represents the mean (n=3) with SD. *$p<0.05$ by student t-test. "#" indicates that all samples
589 treated with OA were significant from the corresponding strain in TSB alone. Data is
590 representative of at least three independent experiments.

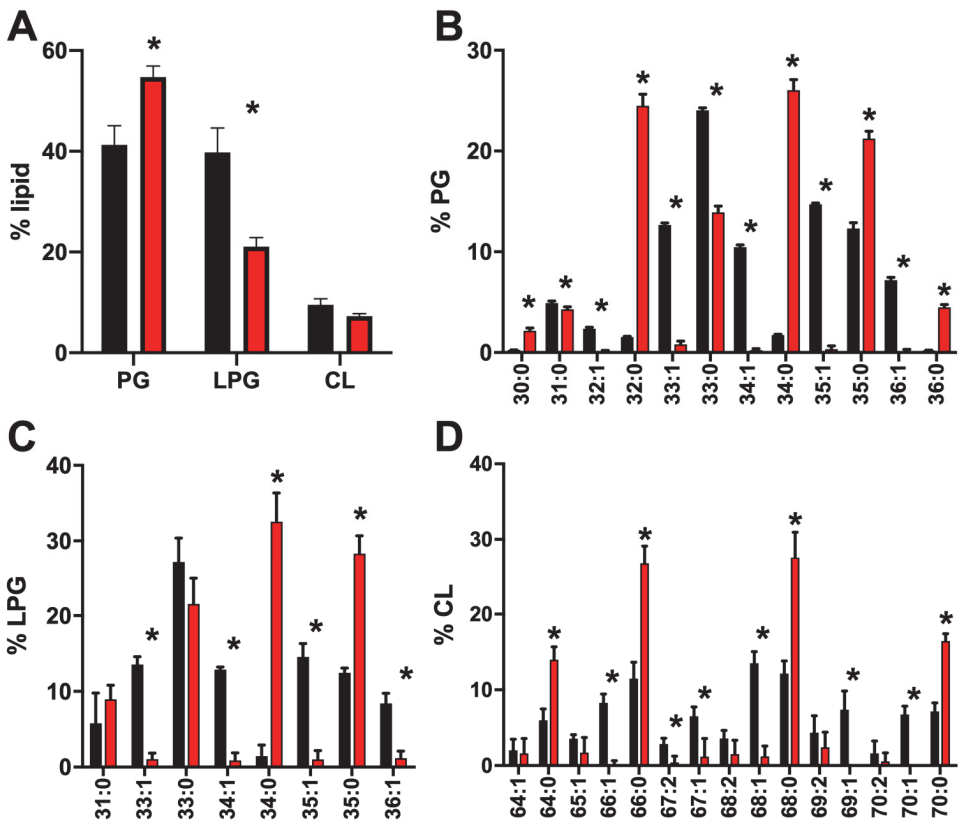

591

592 **Figure 6.** Lipid profile of wildtype (black) and *fakA* mutant (red) grown in 75% mouse skin
593 homogenate. **(A)** Total percent lipid signal of wildtype and *fakA* mutant by class of lipid.
594 Identification of **(B)** phosphatidylglycerol (PG), **(C)** lysyl-PG (LPG), and **(D)** cardiolipin (CL)
595 represented by the percentage of the total from each class. Data represents the mean (n=4) with
596 standard deviation of representative experiment. *$p<0.05$ by student t-test.

597

598 **References**

599 1. Lowy FD. 1998. *Staphylococcus aureus* Infections. New England Journal of Medicine
600 339:520-532.

2. Wertheim HF, Melles DC, Vos MC, van Leeuwen W, van Belkum A, Verbrugh HA, Nouwen JL. 2005. The role of nasal carriage in *Staphylococcus aureus* infections. Lancet Infect Dis 5:751-62.

3. Tong SY, Davis JS, Eichenberger E, Holland TL, Fowler VG, Jr. 2015. *Staphylococcus aureus* infections: epidemiology, pathophysiology, clinical manifestations, and management. Clin Microbiol Rev 28:603-61.

4. Klevens RM. 2007. Invasive Methicillin-Resistant *Staphylococcus aureus* Infections in the United States. JAMA 298:1763.

5. Knox J, Uhlemann AC, Lowy FD. 2015. *Staphylococcus aureus* infections: transmission within households and the community. Trends Microbiol 23:437-44.

6. Chandler CE, Ernst RK. 2017. Bacterial lipids: powerful modifiers of the innate immune response. F1000Research 6:1334.

7. Nguyen MT, Gotz F. 2016. Lipoproteins of Gram-Positive Bacteria: Key Players in the Immune Response and Virulence. Microbiol Mol Biol Rev 80:891-903.

8. Peschel A, Jack RW, Otto M, Collins LV, Staubitz P, Nicholson G, Kalbacher H, Nieuwenhuizen WF, Jung G, Tarkowski A, van Kessel KPM, van Strijp JAG. 2001. *Staphylococcus aureus* Resistance to Human Defensins and Evasion of Neutrophil Killing via the Novel Virulence Factor Mprf Is Based on Modification of Membrane Lipids with l-Lysine. The Journal of Experimental Medicine 193:1067-1076.

9. Ernst CM, Peschel A. 2019. MprF-mediated daptomycin resistance. International Journal of Medical Microbiology doi:10.1016/j.ijmm.2019.05.010.

10. Jiang J-H, Bhuiyan MS, Shen H-H, Cameron DR, Rupasinghe TWT, Wu C-M, Le Brun AP, Kostoulias X, Domene C, Fulcher AJ, McConville MJ, Howden BP, Lieschke GJ,

624 Peleg AY. 2019. Antibiotic resistance and host immune evasion in *Staphylococcus aureus*
625 mediated by a metabolic adaptation. Proceedings of the National Academy of Sciences
626 116:3722-3727.
627 11. Dowds CM, Kornell S-C, Blumberg RS, Zeissig S. 2014. Lipid antigens in immunity. 395.
628 12. Liu Y, Defourny KAY, Smid EJ, Abee T. 2018. Gram-Positive Bacterial Extracellular
629 Vesicles and Their Impact on Health and Disease. Frontiers in Microbiology 9.
630 13. White SW, Zheng J, Zhang Y-M, Rock CO. 2005. THE STRUCTURAL BIOLOGY OF
631 TYPE II FATTY ACID BIOSYNTHESIS. Annual Review of Biochemistry 74:791-831.
632 14. Wang Y, Ma S. 2013. Recent Advances in Inhibitors of Bacterial Fatty Acid Synthesis
633 Type II (FASII) System Enzymes as Potential Antibacterial Agents.
634 doi:10.1002/cmdc.201300209:n/a-n/a.
635 15. Lu H, Tonge PJ. 2008. Inhibitors of FabI, an Enzyme Drug Target in the Bacterial Fatty
636 Acid Biosynthesis Pathway. 41:11-20.
637 16. Omura S. 1976. The antibiotic cerulenin, a novel tool for biochemistry as an inhibitor of
638 fatty acid synthesis. Bacteriol Rev 40:681-97.
639 17. Wang J, Soisson SM, Young K, Shoop W, Kodali S, Galgoci A, Painter R, Parthasarathy
640 G, Tang YS, Cummings R, Ha S, Dorso K, Motyl M, Jayasuriya H, Ondeyka J, Herath K,
641 Zhang C, Hernandez L, Allocco J, Basilio Á, Tormo JR, Genilloud O, Vicente F, Pelaez F,
642 Colwell L, Lee SH, Michael B, Felcetto T, Gill C, Silver LL, Hermes JD, Bartizal K,
643 Barrett J, Schmatz D, Becker JW, Cully D, Singh SB. 2006. Platensimycin is a selective
644 FabF inhibitor with potent antibiotic properties. Nature 441:358-361.

645 18. Parsons JB, Broussard TC, Bose JL, Rosch JW, Jackson P, Subramanian C, Rock CO.
646 2014. Identification of a two-component fatty acid kinase responsible for host fatty acid
647 incorporation by *Staphylococcus aureus*. Proc Natl Acad Sci U S A 111:10532-7.
648 19. Kuhn S, Slavetinsky CJ, Peschel A. 2015. Synthesis and function of phospholipids in
649 *Staphylococcus aureus*. Int J Med Microbiol 305:196-202.
650 20. Parsons JB, Frank MW, Jackson P, Subramanian C, Rock CO. 2014. Incorporation of
651 extracellular fatty acids by a fatty acid kinase-dependent pathway in *Staphylococcus*
652 *aureus*. Molecular Microbiology 92:234-245.
653 21. Sen S, Sirobhushanam S, Johnson SR, Song Y, Tefft R, Gatto C, Wilkinson BJ. 2016.
654 Growth-Environment Dependent Modulation of *Staphylococcus aureus* Branched-Chain
655 to Straight-Chain Fatty Acid Ratio and Incorporation of Unsaturated Fatty Acids. PLOS
656 ONE 11:e0165300.
657 22. Kaiser JC, Sen S, Sinha A, Wilkinson BJ, Heinrichs DE. 2016. The role of two branched-
658 chain amino acid transporters in *Staphylococcus aureus* growth, membrane fatty acid
659 composition and virulence. Molecular Microbiology 102:850-864.
660 23. Singh VK, Hattangady DS, Giotis ES, Singh AK, Chamberlain NR, Stuart MK, Wilkinson
661 BJ. 2008. Insertional inactivation of branched-chain alpha-keto acid dehydrogenase in
662 *Staphylococcus aureus* leads to decreased branched-chain membrane fatty acid content and
663 increased susceptibility to certain stresses. Appl Environ Microbiol 74:5882-90.
664 24. Bose JL, Daly SM, Hall PR, Bayles KW. 2014. Identification of the *Staphylococcus aureus*
665 vfrAB operon, a novel virulence factor regulatory locus. Infect Immun 82:1813-22.
666 25. Krute CN, Rice KC, Bose JL. 2016. VfrB is a key activator of the *Staphylococcus aureus*
667 SaeRS two-component system. doi:10.1128/jb.00828-16:JB.00828-16.

668 26. Ericson ME, Subramanian C, Frank MW, Rock CO. 2017. Role of Fatty Acid Kinase in
669 Cellular Lipid Homeostasis and SaeRS-Dependent Virulence Factor Expression in
670 *Staphylococcus aureus*. MBio 8.
671 27. Demars Z, Bose JL. 2018. Redirection of Metabolism in Response to Fatty Acid Kinase in
672 *Staphylococcus aureus*. Journal of Bacteriology 200.
673 28. Krute CN, Ridder MJ, Seawell NA, Bose JL. 2019. Inactivation of the exogenous fatty acid
674 utilization pathway leads to increased resistance to unsaturated fatty acids in
675 *Staphylococcus aureus*. Microbiology 165:197-207.
676 29. Alnaseri H, Kuiack RC, Ferguson KA, Schneider JET, Heinrichs DE, McGavin MJ. 2018.
677 DNA Binding and Sensor Specificity of FarR, a Novel TetR Family Regulator Required
678 for Induction of the Fatty Acid Efflux Pump FarE in *Staphylococcus aureus*. Journal of
679 Bacteriology 201.
680 30. Bligh EG, Dyer WJ. 1959. A RAPID METHOD OF TOTAL LIPID EXTRACTION AND
681 PURIFICATION. Canadian Journal of Biochemistry and Physiology 37:911-917.
682 31. Koprivnjak T, Zhang D, Ernst CM, Peschel A, Nauseef WM, Weiss JP. 2011.
683 Characterization of *Staphylococcus aureus* Cardiolipin Synthases 1 and 2 and Their
684 Contribution to Accumulation of Cardiolipin in Stationary Phase and within Phagocytes.
685 193:4134-4142.
686 32. Ernst CM, Staubitz P, Mishra NN, Yang S-J, Hornig G, Kalbacher H, Bayer AS, Kraus D,
687 Peschel A. 2009. The Bacterial Defensin Resistance Protein MprF Consists of Separable
688 Domains for Lipid Lysinylation and Antimicrobial Peptide Repulsion. 5:e1000660.

689 33. Parsons JB, Frank MW, Subramanian C, Saenkham P, Rock CO. 2011. Metabolic basis for
690 the differential susceptibility of Gram-positive pathogens to fatty acid synthesis inhibitors.
691 108:15378-15383.
692 34. Braungardt H, Singh VK. 2019. Impact of Deficiencies in Branched-Chain Fatty Acids and
693 Staphyloxanthin in *Staphylococcus aureus*. BioMed Research International 2019:1-8.
694 35. Subczynski WK, Wisniewska A. 2000. Physical properties of lipid bilayer membranes:
695 relevance to membrane biological functions. Acta Biochim Pol 47:613-25.
696 36. Gruszecki WI, Strzałka K. 2005. Carotenoids as modulators of lipid membrane physical
697 properties. Biochimica et Biophysica Acta (BBA) - Molecular Basis of Disease 1740:108-
698 115.
699 37. Mishra NN, Liu GY, Yeaman MR, Nast CC, Proctor RA, McKinnell J, Bayer AS. 2011.
700 Carotenoid-Related Alteration of Cell Membrane Fluidity Impacts *Staphylococcus aureus*
701 Susceptibility to Host Defense Peptides. 55:526-531.
702 38. Mogen AB, Carroll RK, James KL, Lima G, Silva D, Culver JA, Petucci C, Shaw LN, Rice
703 KC. 2017. *Staphylococcus aureus* nitric oxide synthase (saNOS) modulates aerobic
704 respiratory metabolism and cell physiology. Mol Microbiol 105:139-157.
705 39. Lewis AM, Matzdorf SS, Endres JL, Windham IH, Bayles KW, Rice KC. 2015.
706 Examination of the *Staphylococcus aureus* nitric oxide reductase (saNOR) reveals its
707 contribution to modulating intracellular NO levels and cellular respiration. Molecular
708 Microbiology 96:651-669.
709 40. Kiezel-Tsugunova M, Kendall AC, Nicolaou A. 2018. Fatty acids and related lipid
710 mediators in the regulation of cutaneous inflammation. Biochem Soc Trans 46:119-129.

711 41. Delekta PC, Shook JC, Lydic TA, Mulks MH, Hammer ND. 2018. *Staphylococcus aureus*
712 Utilizes Host-Derived Lipoprotein Particles as Sources of Fatty Acids. Journal of
713 Bacteriology 200.
714 42. Hayami M, Okabe A, Kariyama R, Abe M, Kanemasa Y. 1979. Lipid Composition
715 of*Staphylococcus aureus* and Its Derived L-forms. 23:435-442.
716 43. Mishra NN, Bayer AS. 2013. Correlation of Cell Membrane Lipid Profiles with
717 Daptomycin Resistance in Methicillin-Resistant *Staphylococcus aureus*. Antimicrobial
718 Agents and Chemotherapy 57:1082-1085.
719 44. Mukhopadhyay K, Whitmire W, Xiong YQ, Molden J, Jones T, Peschel A, Staubitz P,
720 Adler-Moore J, McNamara PJ, Proctor RA, Yeaman MR, Bayer AS. 2007. In vitro
721 susceptibility of *Staphylococcus aureus* to thrombin-induced platelet microbicidal protein-
722 1 (tPMP-1) is influenced by cell membrane phospholipid composition and asymmetry.
723 Microbiology 153:1187-1197.
724 45. Parsons JB, Yao J, Frank MW, Jackson P, Rock CO. 2012. Membrane Disruption by
725 Antimicrobial Fatty Acids Releases Low-Molecular-Weight Proteins from *Staphylococcus*
726 *aureus*. Journal of Bacteriology 194:5294-5304.
727 46. Lopez MS, Tan IS, Yan D, Kang J, McCreary M, Modrusan Z, Austin CD, Xu M, Brown
728 EJ. 2017. Host-derived fatty acids activate type VII secretion in *Staphylococcus aureus*.
729 Proc Natl Acad Sci U S A 114:11223-11228.
730 47. Tiwari K, Gatto C, Wilkinson B. 2018. Interrelationships between Fatty Acid Composition,
731 Staphyloxanthin Content, Fluidity, and Carbon Flow in the *Staphylococcus aureus*
732 Membrane. Molecules 23:1201.

48. Schurig-Briccio LA, Parraga Solorzano PK, Lencina AM, Radin JN, Chen GY, Sauer JD, Kehl-Fie TE, Gennis RB. 2020. Role of respiratory NADH oxidation in the regulation of *Staphylococcus aureus* virulence. EMBO Rep doi:10.15252/embr.201845832:e45832.
49. Unden G, Bongaerts J. 1997. Alternative respiratory pathways of Escherichia coli: energetics and transcriptional regulation in response to electron acceptors. Biochimica et Biophysica Acta (BBA) - Bioenergetics 1320:217-234.
50. Neumann Y, Ohlsen K, Donat S, Engelmann S, Kusch H, Albrecht D, Cartron M, Hurd A, Foster SJ. 2015. The effect of skin fatty acids on *Staphylococcus aureus*. 197:245-267.
51. Kenny JG, Ward D, Josefsson E, Jonsson I-M, Hinds J, Rees HH, Lindsay JA, Tarkowski A, Horsburgh MJ. 2009. The *Staphylococcus aureus* Response to Unsaturated Long Chain Free Fatty Acids: Survival Mechanisms and Virulence Implications. PLoS ONE 4:e4344.
52. Morvan C, Halpern D, Kénanian G, Hays C, Anba-Mondoloni J, Brinster S, Kennedy S, Trieu-Cuot P, Poyart C, Lamberet G, Gloux K, Gruss A. 2016. Environmental fatty acids enable emergence of infectious *Staphylococcus aureus* resistant to FASII-targeted antimicrobials. 7:12944.
53. Devaiah SP, Roth MR, Baughman E, Li M, Tamura P, Jeannotte R, Welti R, Wang X. 2006. Quantitative profiling of polar glycerolipid species from organs of wild-type Arabidopsis and a phospholipase Dalpha1 knockout mutant. Phytochemistry 67:1907-24.
54. Welti R, Li M, Li W, Sang Y, Biesiada H, Zhou H-E, Rajashekar C, Williams T, Wang X. 2002. Profiling membrane lipids in plant stress response. J Biol Chem 277:31994-32002.
55. Narayanan S, Tamura PJ, Roth MR, Prasad PV, Welti R. 2016. Wheat leaf lipids during heat stress: I. High day and night temperatures result in major lipid alterations. Plant Cell Environ 39:787-803.

56. Brugger B, Erben G, Sandhoff R, Wieland FT, Lehmann WD. 1997. Quantitative analysis of biological membrane lipids at the low picomole level by nano-electrospray ionization tandem mass spectrometry. Proc Natl Acad Sci U S A 94:2339-44.

57. Welti R, Li W, Li M, Sang Y, Biesiada H, Zhou HE, Rajashekar CB, Williams TD, Wang X. 2002. Profiling membrane lipids in plant stress responses. Role of phospholipase D alpha in freezing-induced lipid changes in Arabidopsis. J Biol Chem 277:31994-2002.

58. Singh VK, Sirobhushanam S, Ring RP, Singh S, Gatto C, Wilkinson BJ. 2018. Roles of pyruvate dehydrogenase and branched-chain α-keto acid dehydrogenase in branched-chain membrane fatty acid levels and associated functions in *Staphylococcus aureus*. Journal of Medical Microbiology 67:570-578.

59. Boles BR, Thoendel M, Roth AJ, Horswill AR. 2010. Identification of genes involved in polysaccharide-independent *Staphylococcus aureus* biofilm formation. PLoS One 5:e10146.